Abnormality-aware bone fracture detection and classification using the triple context attention model

Tabassum Nahid Sultana, Asma Parveen
Department of Computer Science and Engineering, Khaja Bandanawaz College of Engineering, Kalaburagi, India

Article Info

Article history:

Received Dec 28, 2023
Revised Mar 8, 2024
Accepted Mar 21, 2024

Keywords:

Attention mechanism
Convolutional neural network
Mislabeling issues
Triple context attention model
Visual attention network

ABSTRACT

In this study, a novel approach is introduced for fracture detection in bone x-ray images, introducing the triple context attention model (TCAN) that combines concentrated extensive convolutional segments with an attention mechanism to enhance positional data. The TCAN model significantly improves fracture recognition accuracy while reducing model complexity. Leveraging a diverse dataset, consistently achieving high accuracy levels across various body parts. By addressing, mislabelling issues, and employing a visual attention network (VAN), to refine the model's performance. The TCAN model emerges as a robust, computationally efficient solution, offering a remarkable average accuracy of 97.86%. This study contributes valuable advancements to medical imaging and diagnostics, providing a highly effective tool for skeletal fracture detection.

Corresponding Author:

Tabassum Nahid Sultana
Department of Computer Science and Applications, Khaja Bandanawaz College of Engineering
Kalaburagi, India
Email: tabassumns_12@rediffmail.com

1. INTRODUCTION

There are 206 bones in the human body in total, and they differ in size, complexity, and structure. The tiniest bones in the human body are located in the ear canal, whereas the biggest bones are found in the femur. Individuals frequently experience lower leg bone fractures [1]. In recent years, there has been a significant increase in the use of machine learning, a method for identifying patterns, for the interpretation of medical imaging. The most reliable predictor was found to be the trait [2]. Healthcare practitioners are greatly helped by the use of this technology in accurately identifying medical disorders and choosing the best course of therapy for their patients. Skeletal fractures can frequently develop without warning, making it crucial to identify them quickly and offer the proper care. There has been a reported rise in bone fractures worldwide, affecting both industrialized and developing nations [3].

To enable the effective sharing of medical pictures, the digital imaging and communications in medicine (DICOM) standard is used. For the goal of helping in the detection of bone fractures, x-ray technology is frequently used in the medical industry. This is because it is quick, affordable, and simple to use. Numerous diseases and injuries can lead to bone fractures. For a therapy to be effective, a prompt and precise diagnosis is required. To assess the features and severity of a fracture, doctors or radiologists frequently request an x-ray examination [4], [5]. It has been discovered that both manual examination and the traditional x-ray fracture detection method are unsuccessful. One of the photos' failure to reveal a fracture to the radiologist might be attributed to an incorrect interpretation of the image as normal, perhaps brought on by exhaustion. An alert is then issued to the attending physician once the x-ray picture has been reviewed by a computer vision system for any anomalies [6].

For identifying bone fractures, three main approaches have been used in earlier studies [7] denoising x-ray pictures, extracting pertinent characteristics, and image classification. Previous studies have concentrated on either a particular anatomical area or a specific type of fracture [8]. An open fracture of the tibia, a fracture of the arm, or a subtle fracture of the femur neck are a few instances of fractures. Finding the precise position of the fracture site was difficult using the approach outlined in the reference [9]. The technology was only capable of correctly determining whether the exhibited bone picture showed a fracture. The knowledge and skills of seasoned medical professionals are required for the detection of fractures in various anatomical locations. Therefore, by accurately identifying bone fractures in various human bone tissues, a pragmatic technique would have advantages. The large variances seen across various bone formations make it difficult to develop a bone accounting system.

By attaining cutting-edge performance levels, deep learning models have shown amazing achievements in a variety of fields, including bioinformatics, computer vision, and medical diagnostics [10]. Deep learning has been shown to have a potential for detecting bone anomalies, although it is only somewhat successful due to its too dependence on deep networks. In their research, [11]-[13] developed a deep convolutional neural network (CNN)-based method for fracture diagnosis. To improve the quality of a picture, preparation techniques are used. By using data augmentation techniques, the dataset's size is increased. A classification model called the Ada-ResNeSt model is used to distinguish between samples of damaged and healthy bones. The accuracy attained is 68.4% on average. The use of x-ray pictures of the humerus bone in a separate research improved the model performance. To make it easier to identify fractures in arm bones, a fracture diagnosis model was created. Three different components make up the main changes. To create a new backbone network to gather additional fractal information, a function pyramid architecture is implemented. The next step in picture preparation entails using an opening approach and modifying the pixel value to effectively boost the contrast of the source images [14]-[16].

The development of a fuzzy c-means approach and the addition of a distance measure to assess structural similarity. This strategy was put into practice to perform picture segmentation. The approach outlined by [16]-[18] uses deep learning methods to identify and categorize different kinds of proximal humerus fractures. Greater tuberosity fractures, surgical neck fractures, 3-part fractures, and 4-part fractures are among the fractures that come under this category. Shoulder radiographs taken from the anterior and posterior are used for the examination. The pre-processing stage comprises downsizing incoming photos to 256×256 pixel size. After that, the preprocessed images are sent into a classifier that makes use of CNN. An accuracy rating of 96% was attained using a dataset of 1,891 images. Here they established the technique for locating abnormalities in the upper extremity bones in their investigation [19]-[21]. A tightly linked convolutional network with 169 layers was used in the approach. The submitted photos are resized to 320×320 pixel dimensions using the scaling procedure. To add more information, the pre-processed photos are randomly inverted and rotated. The photos are put into a convolutional network with 169 layers to enhance the identification of bone anomalies. A 70.5% accuracy was attained on average using the musculoskeletal radiographs (MURA) dataset [22], [23]. The upper extremity bones of the shoulder, forearm, humerus, elbow, wrist, hand, and finger are depicted in more than 40,000 images from various angles in the collection. It is important to recognize that each bone in the context of this investigation is evaluated separately [24].

This research is motivated by the increasing prevalence of skeletal fractures worldwide and the need for accurate detection methods across diverse anatomical regions. Traditional approaches like manual examination and conventional x-ray interpretation face accuracy limitations. To address this, the study employs advanced deep learning techniques, including the triple context attention model (TCAN), to enhance fracture detection accuracy. By utilizing CNN and attention mechanisms, the research aims to provide reliable tools for timely and effective fracture identification in body parts such as the shoulder, humerus, finger, elbow, wrist, forearm, and hand. This work contributes valuable insights into medical diagnostics and improves fracture detection, benefiting both patients and healthcare providers.

- A coordination attention mechanism is designed that enhances fracture recognition accuracy by efficiently incorporating positional data.
- A proposed TCAN approach is designed, which integrates convolutional segments and attention mechanisms, and reduces complexity while improving fracture detection accuracy.
- TCAN's use of positional data and attribute-focused evaluations boosts fracture recognition accuracy, ensuring precise diagnoses in medical imaging.

The research work is organized in this paper as follows: in the first section, a brief overview is given. In the second section proposed methodology is given in which a novel TCAN model is developed. In the third section, the performance analysis is given where the results are displayed in the form of graphs and tables.

2. PROPOSED METHODOLOGY

Considering traditional methods, attention models are used during interlinked connections while overlooking the significance of location data. This challenge results in the accuracy of detection being diminished. However, there also exist models such as the bottleneck attention model and block convolution attention method to retrieve positional data after compression. However, these models can retrieve local connections, although cannot acquire extended dependencies. A coordination attention mechanism was proposed in the existing methodologies that take into consideration positional data that is straight horizontally as well as vertically for connection attention. This method is efficiently implemented for mobile networks that permit wider attention to the positional data while not overworking computations.

Various bone x-ray images are utilized in this study for distinguishing characteristic features along with particular positional data. Hence, using the coordination attention module for this method the accuracy for recognition is enhanced. During the recognition process for these bone x-ray images, the TCAN model is implemented where damaged regions in the image are mislabelled as fractures, this is due to the absence of positional data in the training process. To deal with this challenge the prior existing coordination attention model could be adapted, however, it increases the complexity as well as the parametric dimension of the model decreasing its accuracy. Therefore, we need to resolve this challenge by introducing a TCAN where the proposed model is a combination of concentrated extensive convolutional segments combined with the mentioned attention method. The concentrated convolution has the advantage of recombining the connections while the attention method is flexible to weights. The TCAN model enhances the positional data by focusing on weights for increased dimension for features. Since the weights utilized for this model are distributed, the parametric dimension is also decreased. Using the triple context attention model has enhanced accuracy for the detection of multiple fractures in bone x-ray images.

For the input x-ray images in the TCAN model proposed in this study, there are weight-related evaluations considering channels during the pooling process. However, the proposed model has various convolutional layers that aid in retrieving an increased resolution activation map. Before the coordination attention model channel evaluation, the TCAN model uses pixels for the convolution of the information, the pixel size used for this process is both 1 by 1 as well as 3 by 3. Here, spatial data as well as channel data is enciphered using residual links. Later, modified pooling is performed individually considering length and breadth. The mean of the tensor subset is calculated, then two completely linked convolutional layers are utilized to attain the weights of every particular subset using the mean. These weights are collectively used in the activation map. The combination of attributes causes the activation map with weights to be added according to elements to the initial activation map, this leads to obtaining the final resulting activation map. The TCAN model improvises the focus on the main attributes, decreases the noise in the background that could be found during the object recognition process as well as enhances the accuracy of recognition.

It is required that the proposed model gains traction in various directions and utilizes the positional data. The TCAN model uses an increased resolution activation map attached using the concentrated Extensive convolutional segments as initial input. Pixel dimensions of 1 by 1, as well as 3 by 3, are used, generating y_d. The mean pooling considering length and breadth is performed that attains two activation maps that manifest each direction. This causes the proposed model to improve its concentration of essential attributes in the bone x-ray images as well as use data to represent the attributes. The activation maps are evaluated using the equations listed in (1).

$$a_d^i(i) = (X)^{-1} \sum_{\text{o less than equal to j less than equal to X}} |y_d(i,j) \tag{1}$$

$$a_d^x(x) = (I)^{-1} \sum_{\text{o less than equal to j less than equal to I}} |y_d(k,x) \tag{2}$$

Considering the equations, the channel count is indicated as D. In the pooling process, the length and breadth position value ranges are denoted as I and X. The present position value is given using i and x. The activation maps have receptive areas considering their length and breadth, combined to obtain a dimensional vector of 1 by $2D$. A pixel of resolution 1 by 1 is used through which the vector is passed decreasing its dimensions to D/s. The activation map with decreased dimension is normalized using the batch method and used as input for the sigmoid function. This leads to the activation map having the dimension g as given in (2).

$$g = (X + I) \times D/s \tag{3}$$

Considering this activation map, every element depicts the weight relating to the channel as well as the position spatially, this is utilized in the input activation map. Here the weight grows for attributes that are useful while the unwanted attributes have their weight subdued. In this case, g is evaluated using the following equation given in (4).

$$g = (G_1([a^i, a^x]))\,\partial \quad (4)$$

A sequential operation combined with spatial size is represented using $a^i, a^x]$, where a nonlinear activation function is used and denoted as ∂. The activation map g is transformed into the initial length and breadth implemented by a pixel of size 1 by 1 that gives rise to two activation maps having similar channel counts that are denoted as G_i and G_x. The weights $h^i$and h^x are gathered by using the activation function for length and breadth respectively, these evaluations are performed using (5).

$$h^i = (G_i(g^i)) \times \sigma \quad (5)$$

$$h^x = (G_x(g^x)) \times \sigma \quad (6)$$

In the equations, the activation function Sigmoid is represented as σ. The overload of computation is decreased, also reducing the complexity of the model, a decreasing ratio s is used to limit the size of the channel g. The notations h^i and h^x are the outputs that are enlarged as well and weights are used for computations. These results in the activation map combined with weights for length as well as breadth directions. The TCAN model output z is evaluated using (7).

$$z_d(j,k) = \big(y(j,k)\big) + (h_d^i(j))(h_d^x(k))(y_d(j,k)) \quad (7)$$

A sequential model is used in this study to enhance the accuracy percentage of bone x-racy images. Here, a visual attention network (VAN) is introduced, this deep learning method is used as a transformer for image processing that works as an attention model. The accuracy of classification is seen to be high during the performance of VAN as well as takes care of all the normal tasks of classification relating to images. Considering bone x-ray image datasets, there exists diversity in dimensions that happens due to capturing distance, resources used to capture images, and individual photographers. The VAN model splits the input image and rejoins the images, showing an adaptable skill to manage the diversity in these x-rays that contain various dimensions and sizes. The VAN model is pre-trained in this study using bone x-ray image datasets as well as refined using deep learning methodologies of transfer learning for bone x-ray image classification. The VAN model has three phases, namely local feature embedding, transformer input encoder, and lastly multi-layer perceptron. Table 1 (see in Appendix) shows algorithm workflow.

3. PERFORMANCE ANALYSIS

The TCAN model, as proposed, undergoes assessment using the current cutting-edge techniques found in the MURA database. This assessment encompasses various body parts such as the shoulder, humerus, finger, elbow, wrist, forearm, and hand. The outcomes of this evaluation are presented through graphical representations and tables.

3.1. Dataset details

To prepare for and manage tests, the MURA database [25] is used. The dataset is regarded as one of the most complete public archives of radiographic pictures in general and is largely accepted as the largest publicly available collection of bone anomalies. The dataset comprises 5,915 abnormal and 9,067 normal upper extremity MURA images. The shoulder, humerus, elbow, forearm, wrist, hand, and finger are explicitly included in the scans along with other anatomical parts.

3.2. Results

The proposed TCAN model is carried out in two stages detection and classification. The proposed TCAN model is structured around a two-stage methodology focusing on both detection and classification tasks. This sequential approach allows for a comprehensive analysis, ensuring efficient identification and accurate categorization of the targeted elements within the dataset.

3.3. Detection

In the context of the TCAN model, the term "detection" refers to the initial phase where the system identifies or localizes specific objects or patterns within the input data. This stage involves pinpointing the presence and location of relevant elements of interest, such as anatomical structures or abnormalities, within images or datasets. Detection encompasses recognizing and outlining regions or points of significance, often through techniques like object localization or segmentation. In medical imaging, for instance, this could involve identifying particular body parts, lesions, fractures, or anomalies within x-rays or scans. Figure 1 shows the detection of bone fracture.

Table 1. Algorithm workflow

Steps	Algorithms

Step 1	If (TCAN_Model not initialized)
	Initialize TCAN_Model architecture
	Setup TCAN_Layer for feature enhancement
	Add convolutional layers, max-pooling, and relevant components
	Train TCAN_Model using bone x-ray image dataset
	else
	TCAN_Model already initialized, proceed to the next step

Step 2	TCAN Feature Extraction
	if (Input_Image not preprocessed)
	Pre-process bone x-ray images for fracture detection
	Split input x-ray images into non-overlapping segments
	else
	Input images already pre-processed, proceed to the next step
	if (TCAN_Model not applied)
	Pass image segments through TCAN_Model
	Utilize TCAN to extract essential features, enhancing positional data
	else
	TCAN_Model already applied, proceed to the next step

Step3:	if (VAN_Model not initialized)
	Initialize VAN_Model architecture for image processing and classification
	Include VAN_Layer for attention-based feature enhancement
	Add dense layers, dropout, and softmax activation for classification
	Train VAN_Model using bone x-ray image dataset
	else
	VAN_Model already initialized, proceed to the next step

Step 4:	Combining TCAN and VAN
	if (Features_not_combined)
	Combine feature-enhanced output from TCAN with VAN_Model
	Ensure positional data is retained in the combined features
	else
	Features already combined, proceed to the next step

Step 5:	Batch Normalization
	if (Batch_Normalization_not_applied)
	Apply batch normalization to the combined model to speed up learning
	Normalize the output to prevent overfitting
	else
	Batch normalization has already been applied, proceed to the next step

Step 6	Fracture Detection
	if (Fracture_Detection_not_performed)
	Use the combined TCAN-VAN model to detect fractures in x-ray images
	Recognize fractures in various body parts (e.g., shoulder, arms, hip, chest, legs)
	else:
	Fracture detection has already been performed, proceed to the next step

Step 7:	Model Evaluation
	if (Evaluation_not_completed)
	Evaluate model performance on a test dataset
	Calculate accuracy, precision, recall, F1-score, and other relevant metrics
	else:
	Evaluation already completed, proceed to next step

Figure 1 Detection of bone fracture

3.4. Classification

The table presents a comparative analysis of various CNN architectures for the detection of fractures in different body parts, including the shoulder, humerus, finger, and elbow. Notably, the TCAN model exhibits exceptional accuracy across all body parts, with the highest accuracy achieved in detecting finger fractures (96.6%) and particularly impressive results in humerus detection (97.84%). Inception and InceptionResNetV2 also perform in an average manner, showcasing high accuracy percentages on most body parts. MobileNet stands out with perfect accuracy in identifying humerus fractures. DenseNet201 exhibits variable performance across different body regions. Neural architecture search network (NASNET)0Mobile and Xception deliver robust and consistent accuracy. Figure 2 shows the bone fracture classification.

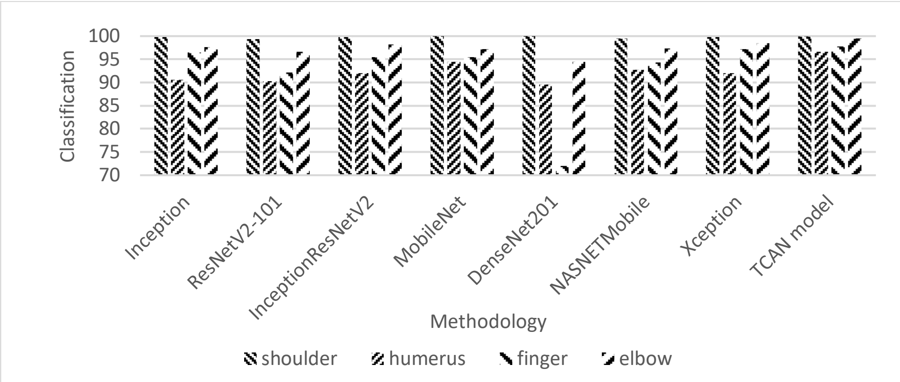

Figure 2. Bone fracture classification

In this analysis of various CNN architectures for the detection of fractures in the wrist, forearm, and hand, the TCAN model is consistently the top-performing model across all body parts. It achieves remarkably high accuracy percentages, with the highest accuracy observed in wrist detection (99.86%) and impressive results in hand detection (99.72%). Inception, MobileNet, and Xception also exhibit strong accuracy levels and are competitive choices for fracture detection, especially in the wrist and hand. ResNetV2-101, InceptionResNetV2, DenseNet201, and NASNETMobile, display varying degrees of accuracy across different body parts. Overall, the TCAN model emerges as a robust and reliable choice for accurate fracture detection in the wrist, and forearm.

3.5. Comparative analysis

In our comparative analysis, we observed remarkable improvements in fracture classification and detection accuracy with the introduction of our proposed TCAN. Our meticulous comparative analysis revealed notable advancements in fracture classification and detection accuracy, underscoring the efficacy and impact of integrating the innovative TCAN. The TCAN model's introduction substantially improved the precision and reliability of identifying fractures, signifying promising potential in medical imaging applications.

3.5.1. Detection

The table provides data on three different bone types: shoulder, humerus, and finger, with scores in TCAN and improvisation. Notably, while the shoulder and finger bones have decent existing conditions, their improvisation percentages are relatively high at 6.0% and 7.76%, respectively. In contrast, the humerus stands out with the highest existing condition score and the lowest improvisation percentage at 5.10%. This suggests that the humerus is the healthiest and least adaptable of the three bones, while the shoulder and finger have more room for improvement or improvisation in their condition. Table 2 shows the improvisation of the existing model for detection.

Table 2. Improvisation of the existing model for detection

Bone	Existing	TCAN	Improvisation (%)
Shoulder	81	87	6.0
Humerus	84.72	89.82	5.10
Finger	78.51	86.27	7.76
Elbow	82.97	87.56	4.59

3.5.2. Classification

Across various body parts, TCAN exhibited significant enhancements, achieving the highest accuracy gain of 9.42% in forearm fracture detection, followed by a 4.87% improvement in humerus detection. Notably, TCAN consistently outperformed the existing system (ES) in all categories, showcasing its effectiveness in accurately identifying fractures. The average accuracy improvement across all body parts was an impressive 2.15%, reinforcing TCAN's reliability in fracture detection tasks. Table 3 shows the classification improvisation.

Table 3. Classification improvisation

	ES	Proposed system (PS)	Improvisation (%)
Shoulder	99.82	99.9	0.0801122
Humerus	92.01	96.6	4.86719
Finger	97.18	97.84	0.676854
Elbow	98.5	99.57	1.08043

4. CONCLUSION

In conclusion, our research presents a novel and effective approach to fracture detection in bone x-ray images through the innovative TCAN. By combining concentrated extensive convolutional segments with an attention mechanism, TCAN significantly enhances the accuracy of fracture recognition while simultaneously reducing model complexity. Our comprehensive evaluation across various body parts demonstrates the consistent and better performance of TCAN, resulting in high accuracy levels in fracture detection. The incorporation of a VAN further refines the model's capabilities, addressing mislabelling challenges in fracture identification. TCAN emerges as a robust and computationally efficient solution for skeletal fracture detection. This research contributes significantly to the field of medical imaging and diagnostics, providing a powerful tool that can greatly assist healthcare professionals in prompt and accurate fracture diagnosis. Our work underscores the potential of deep learning models in medical applications and the importance of addressing challenges in fracture detection to improve patient care and outcomes.

REFERENCE

[1] K. C. Santos, C. A. Fernandes, and J. R. Costa, "Feasibility of bone fracture detection using microwave imaging," *IEEE Open Journal of Antennas and Propagation*, vol. 3, pp. 836–847, 2022, doi: 10.1109/OJAP.2022.3194217.

[2] A. Kheaksong, P. Sanguansat, P. Samothai, T. Dindam, K. Srisomboon, and W. Lee, "Analysis of modern image classification platforms for bone fracture detection," in *2022 6th International Conference on Information Technology (InCIT)*, IEEE, Nov. 2022, pp. 471–474, doi: 10.1109/InCIT56086.2022.10067836.

[3] P. Samothai, P. Sanguansat, A. Kheaksong, K. Srisomboon, and W. Lee, "The evaluation of bone fracture detection of YOLO series," in *2022 37th International Technical Conference on Circuits/Systems, Computers and Communications (ITC-CSCC)*, IEEE, Jul. 2022, pp. 1054–1057, doi: 10.1109/ITC-CSCC55581.2022.9895016.

[4] R. S. Upadhyay and P. Tanwar, "A review on bone fracture detection techniques using image processing," in *2019 International Conference on Intelligent Computing and Control Systems (ICCS)*, IEEE, 2019, pp. 287–292, doi: 10.1109/ICCS45141.2019.9065874.

[5] R. Vijayakumar and G. Gireesh, "Quantitative analysis and fracture detection of pelvic bone X-ray images," in *2013 Fourth International Conference on Computing, Communications and Networking Technologies (ICCCNT)*, IEEE, Jul. 2013, pp. 1–7, doi: 10.1109/ICCCNT.2013.6726590.

[6] T. C. Anu, M. S. Mallikarjunaswamy, and R. Raman, "Detection of bone fracture using image processing methods," *International Journal of Computer Applications*, pp. 6–9, 2015.

[7] G. Moon, S. Kim, W. Kim, Y. Kim, Y. Jeong, and H.-S. Choi, "Computer aided facial bone dracture diagnosis (CA-FBFD) system based on object detection model," *IEEE Access*, vol. 10, pp. 79061–79070, 2022, doi: 10.1109/ACCESS.2022.3192389.

[8] O. Bandyopadhyay, A. Biswas, and B. B. Bhattacharya, "Long-bone fracture detection in digital X-ray images based on digital-geometric techniques," *Computer Methods and Programs in Biomedicine*, vol. 123, pp. 2–14, 2016, doi: 10.1016/j.cmpb.2015.09.013.

[9] C. Z. Basha, M. R. K. Reddy, K. H. S. Nikhil, P. S. M. Venkatesh, and A. V. Asish, "Enhanced computer aided bone fracture detection employing x-ray images by Harris corner technique," in *2020 Fourth International Conference on Computing Methodologies and Communication (ICCMC)*, IEEE, Mar. 2020, pp. 991–995, doi: 10.1109/ICCMC48092.2020.ICCMC-000184.

[10] N. D. Hoang and Q. L. Nguyen, "A novel method for asphalt pavement crack classification based on image processing and machine learning," *Engineering with Computers*, vol. 35, no. 2, pp. 487–498, 2019, doi: 10.1007/s00366-018-0611-9.

[11] F. Uysal, F. Hardalaç, O. Peker, T. Tolunay, and N. Tokgöz, "Classification of shoulder x-ray images with deep learning ensemble models," *Applied Sciences*, vol. 11, no. 6, Mar. 2021, doi: 10.3390/app11062723.

[12] S. H. Sreedhara, V. Kumar, and S. Salma, "Efficient big data clustering using adhoc fuzzy C means and auto-encoder CNN," in *Inventive Computation and Information Technologies*, vol. 563, 2023, pp. 353–368, doi: 10.1007/978-981-19-7402-1_25.

[13] P. Pujar, A. Kumar, and V. Kumar, "Efficient plant leaf detection through machine learning approach based on corn leaf image classification," *IAES International Journal of Artificial Intelligence (IJ-AI)*, vol. 13, no. 1, pp. 1139–1148, 2024, doi: 10.11591/ijai.v13.i1.pp1139-1148.

[14] S. Beyaz, K. Açici, and E. Sümer, "Femoral neck fracture detection in X-ray images using deep learning and genetic algorithm approaches," *Joint Diseases and Related Surgery*, vol. 31, no. 2, pp. 175–183, 2020, doi: 10.5606/EHC.2020.72163.

[15] P. Tobler *et al.*, "AI-based detection and classification of distal radius fractures using low-effort data labeling: evaluation of applicability and effect of training set size," *European Radiology*, vol. 31, no. 9, pp. 6816–6824, 2021, doi: 10.1007/s00330-021-07811-2.
[16] D. H. Kim and T. MacKinnon, "Artificial intelligence in fracture detection: transfer learning from deep convolutional neural networks," *Clinical Radiology*, vol. 73, no. 5, pp. 439–445, 2018, doi: 10.1016/j.crad.2017.11.015.
[17] H. Y. Chen *et al.*, "Application of deep learning algorithm to detect and visualize vertebral fractures on plain frontal radiographs," *PLoS ONE*, vol. 16, no. 1, 2021, doi: 10.1371/journal.pone.0245992.
[18] C. Szegedy, V. Vanhoucke, S. Ioffe, J. Shlens, and Z. Wojna, "Rethinking the inception architecture for computer vision," *arXiv-Computer Science*, pp. 1-10, Dec. 2015, doi: 10.48550/arXiv.1512.00567.
[19] K. He, X. Zhang, S. Ren, and J. Sun, "Identity mappings in deep residual networks," in *Computer Vision – ECCV 2016 (ECCV 2016)*, 2016, pp. 630–645, doi: 10.1007/978-3-319-46493-0_38.
[20] C. Szegedy, S. Ioffe, V. Vanhoucke, and A. Alemi, "Inception-v4, inception-ResNet and the impact of residual connections on learning," *Proceedings of the AAAI Conference on Artificial Intelligence*, vol. 31, no. 1, pp. 4278–4284, Feb. 2017, doi: 10.1609/aaai.v31i1.11231.
[21] A. G. Howard *et al.*, "MobileNets: Efficient convolutional neural networks for mobile vision applications," *arXiv-Computer Science*, pp. 1-9, Apr. 2017, doi: 10.48550/arXiv.1704.04861.
[22] G. Huang, Z. Liu, L. V. D. Maaten, and K. Q. Weinberger, "Densely connected convolutional networks," *arXiv-Computer Science*, pp. 1-9, Aug. 2016, doi: 10.48550/arXiv.1608.06993.
[23] B. Zoph, V. Vasudevan, J. Shlens, and Q. V. Le, "Learning transferable architectures for scalable image recognition," in *2018 IEEE/CVF Conference on Computer Vision and Pattern Recognition*, IEEE, Jun. 2018, pp. 8697–8710, doi: 10.1109/CVPR.2018.00907.
[24] F. Chollet, "Xception: Deep learning with depthwise separable convolutions," *arXiv-Computer Science*, pp. 1-8, Oct. 2016, doi: 10.48550/arXiv.1610.02357
[25] P. Rajpurkar *et al.*, "MURA: Large dataset for abnormality detection in musculoskeletal radiographs," *arXiv-Physics*, pp. 1-10, Dec. 2017, doi: 10.48550/arXiv.1712.06957.

BIOGRAPHIES OF AUTHORS

Tabassum Nahid Sultana received Bachelor of Engineering and Master Degree from VTU Belagavi. Presently she is a Ph.D. research scholar in the Research Centre, KBN College of engineering, Kalaburagi, affiliated to Visvesvaraya Technological University, Belagavi. Her current research area is digital image processing and machine learning. She can be contacted at this email: tabassumns_12@rediffmail.com.

Dr. Asma Parveen got graduated in Electrical Engineering, in 1993 and completed post-graduation in Computer Science and Engineering in 2004 and in 2016. She was awarded Ph.D. in Computer Science and Engineering. She has published many research papers in leading international journals and conference proceedings. She can be contacted at email: drasma.cse@gmail.com.